

Surface Plasmon Resonance and Tamm Plasmon



Submitted by:

Dinesh Beniwal 1811061

Supervised by: Dr. Ritwik Das

Department of Physics

**National Institute of Science Education and Research,
Bhubaneswar**

Contents

List of Figures	ii
Abstract	iv
1 Surface Plasmon Resonance	1
1.1 Theory	1
1.1.1 Plasmonics	1
1.1.2 Surface plasmons	1
1.1.3 Excitation of the SP wave	3
1.2 Experimental Setup	4
1.2.1 Apparatus	4
1.2.2 Method-A	4
1.2.3 Method-B	5
1.3 Results and Discussion	6
1.3.1 Calculation of refractive index of prism	6
1.3.2 SPR (Method-A)	6
1.3.3 SPR (Method-B)	6
1.3.4 Sources of Error	8
1.4 Conclusion	9
2 Tamm Plasmon	10
2.1 Theory	10
2.1.1 Optical Tamm states (OTSs)	10
2.2 Experimental Setup	11
2.2.1 Apparatus	11
2.3 Results and Discussion	12
2.3.1 Tamm plasmon for p-polarised light	12
2.3.2 Tamm plasmon for s-polarised light	12
2.4 Conclusion	12
References	17

List of Figures

1.1	Illustration of a surface plasmon (SP) propagating at a metal-dielectric interface. (a) A schematic of a SP propagating in the x direction with electric and magnetic field components shown. (b) Evanescent decay of the field component that is perpendicular to the interface into both the metal and the dielectric [5]	2
1.2	Sketch of impinging waves on a metallic film for exciting the SP wave in the Kretschmann configuration. The wave of the wave vector \vec{k}_3 travels through the glass prism and creates a wavevector component k_{3x} large enough to excite the SP wave which is launched at the gold/air interface. The wave of the wavevector \vec{k}_2 is unable to couple with the SP wave. This coupling only occurs for p-polarized waves (electric field within the plane of incidence which in our case coincides with the plane of the figure).[4]	3
1.3	Optical setup for measuring the plasmon extinction. Monochromatic p-polarized light impinges on a prism in a total reflection configuration. An ultrathin gold film (thickness 50 nm) is placed on the prism so that it collects the evanescent waves produced by the total reflection and the SP wave is launched at the gold/air interface if the angle is set at a given value. The light intensity reflected by the prism is measured with the photodiode and goes through a minimum when the coupling with the plasmon wave occurs.[4]	5
1.4	Deviation angle vs incident angle	6
1.5	Surface plasmon extinction curve for a gold/air interface measured at a wavelength of 633nm. The graph shows the reflected intensity plotted versus θ_{int} as obtained with relation 1.6	7
1.6	Surface plasmon extinction curve. The graph shows the reflected intensity plotted versus λ at the incident angle ($\alpha = 26.5924^\circ$)	7
1.7	Surface plasmon extinction curve. The graph shows the reflected intensity plotted versus λ at the different incident angle	8
1.8	λ vs the incident angle (α). Blue line shows the theoretical plot(ref.[2]) whereas red data points shows the experimental results.	8
2.1	imulated spectrum of metal coating on PhC formfigure.... configuration. Reflection (Black curve), transmission (Red curve) and PhC reflection (Grey curve) curves	10
2.2	Experimental setup for the observation of Tamm states	11
2.3	Metal coated DBR spectrum for 10° incident angle(for p-polarization)	13
2.4	Metal coated DBR spectrum for 20° incident angle(for p-polarization)	13
2.5	Metal coated DBR spectrum for 30° incident angle(for p-polarization)	13
2.6	Metal coated DBR spectrum for 40° incident angle(for p-polarization)	14

2.7	Metal coated DBR spectrum for 50° incident angle(for p-polarization) . . .	14
2.8	Metal coated DBR spectrum for 20° incident angle(for s-polarization) . . .	15
2.9	Metal coated DBR spectrum for 30° incident angle(for s-polarization) . . .	15
2.10	Metal coated DBR spectrum for 40° incident angle(for s-polarization) . . .	15
2.11	Metal coated DBR spectrum for 50° incident angle(for s-polarization) . . .	16

Abstract

The surface plasmon wave is a surface wave confined at the interface between a dielectric and a metal. We described a series of experiments designed to provide insights into the fundamental properties of surface plasmon resonance in this report. An important part of the experiment involves the excitation of the plasmon resonance by using a He-Ne laser in the Kretschmann configuration, with the gold active film embedded in a prism of glass. An accurate measurement of the plasmon extinction angle is performed and the measurement is compared to the theoretical prediction. This experiment allows accurate determination of the angle of plasmon extinction and discussion of the principles of biosensors based on the SPR. A slight modification (addition of supercontinuum laser) allowed the observation of wavelengths which satisfies the momentum conservation condition.

Second part of the experiment contains the study of Tamm plasmon. Beauty of Tamm plasmon is that it can be observed for both s and p-polarisation. Here Tamm states localisation was achieved via an appropriate experimental setup. Tamm state was obtained for a metal coated DBR and the variation of its wavelength with the angle of incidence was observed. Simulation of Tamm states was skipped as it was completed as earlier lab projects.

Chapter 1

Surface Plasmon Resonance

1.1 Theory

1.1.1 Plasmonics

In a conductive material, such as noble metals, a plasmon is a collective oscillation of free electrons. When an external electric field is applied to fixed ions in a metal, the negative charged electrons move with respect to the positive charged cores. This displacement of electrons leads them to oscillate at the plasma frequency once the electric field is removed [1].

A **plasmon** is a quasi-particle that characterises the quantum of this plasma oscillation, or the oscillating displacement between positive and negative plasma particles. It describes the motion of a group of electrons. Most of the features of plasmons may be obtained simply from Maxwell's equations since they represent the quantization of classical plasma oscillations. The excitation of a plasmon is referred to as **plasmon resonance** [3]. The study of these light-matter interactions is known as **plasmonics**.

1.1.2 Surface plasmons

SPs are coherent electron oscillations that occur at the interface between any two materials, such as a metal-dielectric interface, where the real component of the dielectric function changes sign across the interface. A thin conductive and nonconductive layer must be present, with the charge carriers confined in the conductive layer. As a result of their displacement, a restoring force will develop. SPs are coherent electron oscillations that occur at the interface between any two materials, such as a metal-dielectric interface, where the real part of the dielectric function changes sign across the interface. A thin conductive and nonconductive layer is required, with the charge remaining. In the conductive layer, carriers are trapped. As a result of their displacement, a restoring force emerges will intensify.

Bulk plasmon resonance, surface plasmon resonance (SPR), and localised surface plasmon resonance are the three forms of plasmons that may be identified (LSPR).

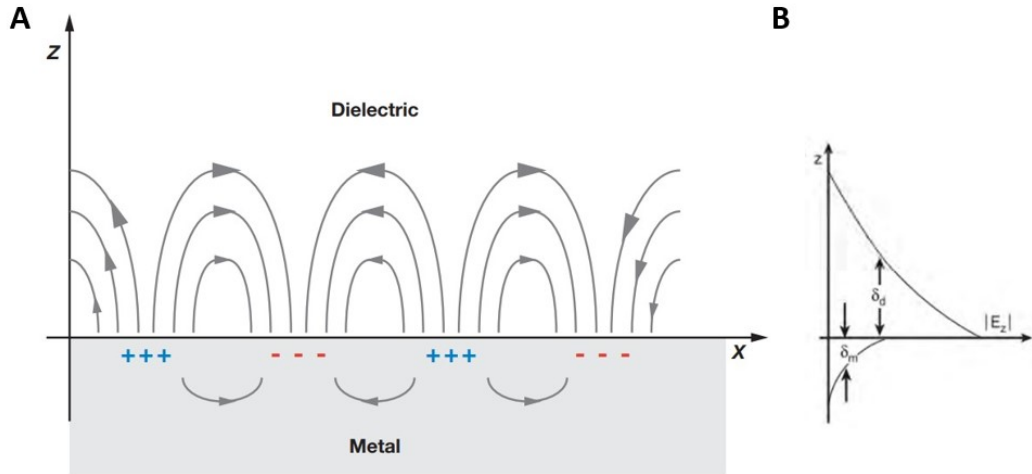


FIGURE 1.1: Illustration of a surface plasmon (SP) propagating at a metal-dielectric interface. (a) A schematic of a SP propagating in the x direction with electric and magnetic field components shown. (b) Evanscent decay of the field component that is perpendicular to the interface into both the metal and the dielectric [5]

The distinction between propagating and confined surface plasmons is illustrated in Figure 1.1(A). Plasmons propagate in the x- and y-directions along the metal-dielectric interface for distances on the order of tens to hundreds of microns, and decay evanescently in the z-direction with $1/e$ decay lengths (Figure 1.1(B)) on the scale of 200 nm in the case of surface plasmon polaritons. Shifts in the plasmon resonance state result from the interaction of the metal surface-confined EM wave with a molecular surface layer of interest, which may be detected in three modes: (a) angle resolved, (b) wavelength shift, and (c) imaging. The reflectance of light from the metal surface is measured as a function of angle of incidence (at constant wavelength) or wavelength in the first two modes (at constant angle of incidence). The third approach probes a two-dimensional section of the material with light of constant wavelength and incidence angle, mapping the reflectivity of the surface as a function of location [5].

The optical evanescent wave is intrinsically coupled to a second evanescent wave on the dielectric side of the interface, and this coupling results in the SP wave. As a consequence, any change in the dielectric medium close to the interface that affects the optical index will modify the propagation of the plasmon wave.

Medium 1 is homogeneous, isotropic and metallic with dielectric function $\epsilon_1(\omega)$ and has a plane interface at $z = 0$ with medium 2 which is a homogeneous and isotropic dielectric. The dielectric function $\epsilon_2(\omega)$ is a real and positive function. As far as metal is concerned, we will consider gold whose dielectric function can be crudely approximated with the Drude–Sommerfeld model that takes into account the free electrons of the metal. In that approach, $\epsilon_1(\omega)$ is given by

$$\epsilon_1 = 1 - \frac{\omega_P^2}{\omega^2} \quad (1.1)$$

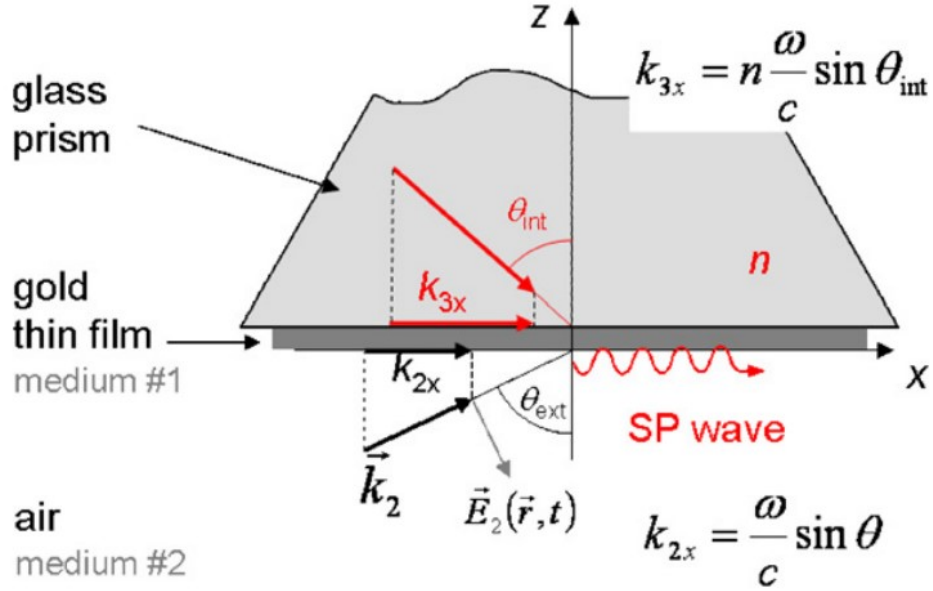


FIGURE 1.2: Sketch of impinging waves on a metallic film for exciting the SP wave in the Kretschmann configuration. The wave of the wave vector \vec{k}_3 travels through the glass prism and creates a wavevector component k_{3x} large enough to excite the SP wave which is launched at the gold/air interface. The wave of the wavevector \vec{k}_2 is unable to couple with the SP wave. This coupling only occurs for p-polarized waves (electric field within the plane of incidence which in our case coincides with the plane of the figure). [4]

Only waves with their electric field polarized within the plane of incidence (p-polarization, see Figure 1.2) are solutions and the electric fields in media 1 and 2 are surface waves characterized by decay lengths and $1/k_{1z}$, $1/k_{2z}$ and a wavevector parallel to the interface which has equal values for the two waves $k_{1x} = k_{2x} = k_x$. From the dispersion equations written in each of the two media, and from the boundary conditions applied to the electric field \vec{E} and electric displacement , the dispersion equation of the SP wave is derived and written as

$$k_x^2 = \frac{\omega^2}{c^2} \cdot \frac{\epsilon_1(\omega) \cdot \epsilon_2(\omega)}{\epsilon_1(\omega) + \epsilon_2(\omega)} \quad (1.2)$$

$$k_{1z}^2 = \frac{\omega^2}{c^2} \cdot \frac{\epsilon_1^2(\omega)}{\epsilon_1(\omega) + \epsilon_2(\omega)} \quad (1.3)$$

$$k_{2z}^2 = \frac{\omega^2}{c^2} \cdot \frac{\epsilon_2^2(\omega)}{\epsilon_1(\omega) + \epsilon_2(\omega)} \quad (1.4)$$

[4] The complete derivation can be found in the Appendix of ref.[4]

1.1.3 Excitation of the SP wave

SP waves are eigenmodes of surface waves, and the most common way to excite them is by coupling them to an external beam of light. It is necessary to conserve both the energy ($\hbar\omega$) and the momentum ($\hbar\vec{k}$) of the excitation wave in order to couple two electromagnetic waves. The wave is totally reflected and generates an evanescent wave

on the other side of the interface (in the gold medium in Figure 1.2). If θ_{int} is the incidence angle as depicted on Figure 1.2, the dispersion relation is written as

$$k \cdot \sin \theta_{int} = \frac{\omega}{c} \cdot n \quad (1.5)$$

where n is the refractive index of prism. Therefore the condition for coupling the excitation wave with the SP wave is obtained by combining relations (1.2) and (1.5):

$$(n \sin(\theta_{int}))^2 = \frac{\epsilon_1(\omega) \cdot \epsilon_2(\omega)}{\epsilon_1(\omega) + \epsilon_2(\omega)} \quad (1.6)$$

[4]

1.2 Experimental Setup

Experimental setup is described in the Figure 1.3. This experiment used two different method to observe the SPR.

1.2.1 Apparatus

- He-Ne polarised laser
- Super continuum laser
- Polarised beam splitter
- Prism and glycerin
- Gold film
- Detector
- Rotating stage

1.2.2 Method-A

For the first method a polarized He-Ne laser ($\lambda = 633nm$) was used as shown in Figure 1.3. This polarized light then passed through polarized beam splitter(instead of half-wave plate in Figure 1.3) to ensure the p-polarization output for the experiment.

A high-index equilateral prism is used which has refractive index $n = 1.532$ for $\lambda = 633nm$ (calculated using angle of minimum deviation method described in section 3).

Gold film (30nm thick) was adapted on one side of the prism with glycerin($n = 1.4722$). This will definitely cause errors in the experiment but we have to take it as experimental limitation. A manual rotation stage with an accuracy of 0.1° is used for measuring the angle θ_{ext} defined in Figure 1.3. The prism is positioned on the stage so that the 180° angle corresponds to the laser beam being back reflected to the laser. This allows us to directly measure the angle marked θ_{ext} in Figure 1.3(b). The value of θ_{int} is obtained

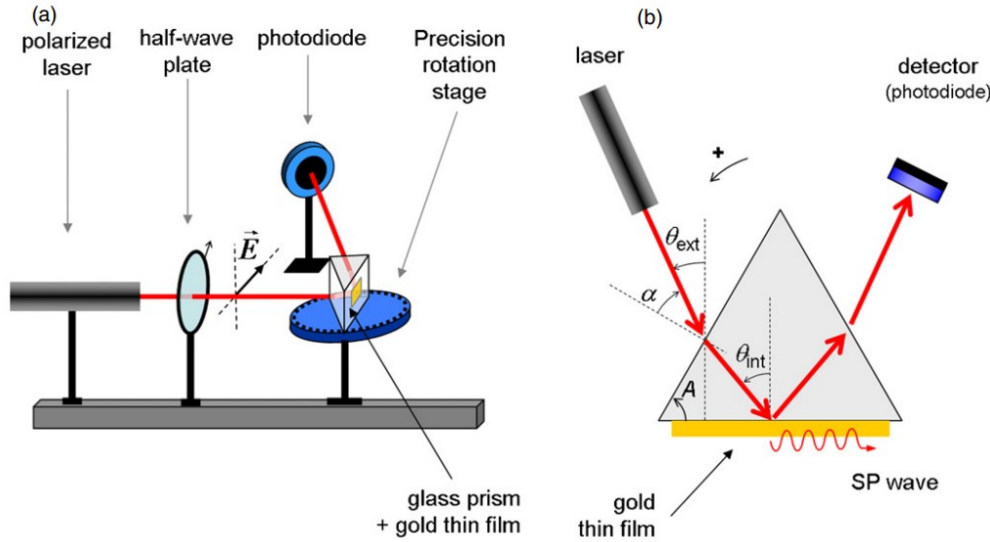


FIGURE 1.3: Optical setup for measuring the plasmon extinction. Monochromatic p-polarized light impinges on a prism in a total reflection configuration. An ultrathin gold film (thickness 50 nm) is placed on the prism so that it collects the evanescent waves produced by the total reflection and the SP wave is launched at the gold/air interface if the angle is set at a given value. The light intensity reflected by the prism is measured with the photodiode and goes through a minimum when the coupling with the plasmon wave occurs..[4]

by the following relation,

$$\theta_{int} = \sin^{-1}(\sin(\theta_{ext} - A)/n) + A \quad (1.7)$$

Angle A is the angle of the prism indicated in Figure 1.3(b) and has been taken as 60° . And the relation between incident angle (α) and θ_{ext} is given as

$$\alpha = 60 - \theta_{ext} \quad (1.8)$$

The reflected beam is collected with a reversed biased photodiode and its intensity can be read with a multimeter.

1.2.3 Method-B

For the first method a supercontinuum laser ($\lambda = [400 - 2100]nm$) was used as shown in Figure 1.3. This light then passed through half-wave plate and a polarized beam splitter to ensure the p-polarization output for the experiment. Gold film (15nm thick) was adapted on one side. The reflected beam is collected with spectrometer. Rest of the experimental components were same as Method-A.

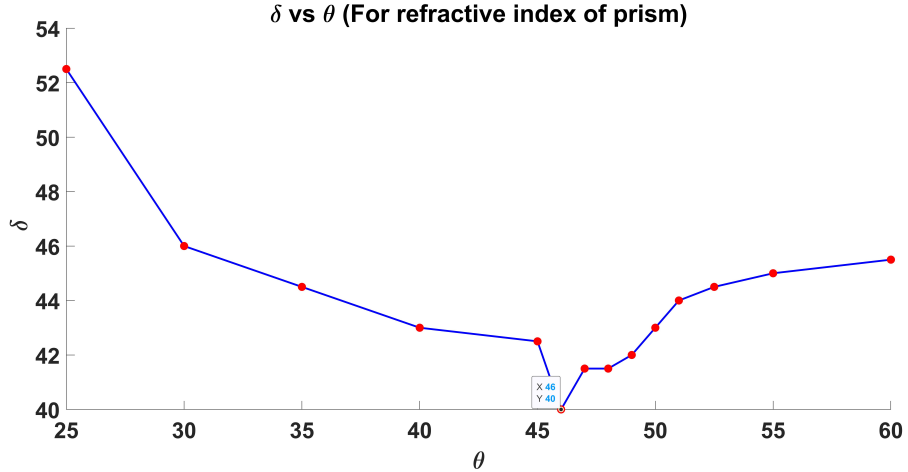


FIGURE 1.4: Deviation angle vs incident angle

1.3 Results and Discussion

1.3.1 Calculation of refractive index of prism

We constructed a table with various values of angle of incidence of light falling on a prism and angle of deviation determined (Figure 1.4). Then the refractive index formula using angle of prism and deviation is used to find the refractive index of the material of the prism.

Refractive index formula

$$n = \frac{\sin((A + \delta_m)/2)}{\sin(A/2)} \quad (1.9)$$

From the Figure 4 the minimum deviation angle was found 40° and the calculated refractive index was $n = 1.5321$.

1.3.2 SPR (Method-A)

Figure 1.5 presents the results obtained with Method-A. The reflected intensity measured with the photodiode has been recorded manually as a function of the incident angle(α) (angle defined in Figure 1.3(b)). The relevant variable for plotting the evolution of the reflected intensity is defined by equation (1.6) and is the internal angle θ_{int} . It is given by formula (1.7 and 1.8). The signature of the plasmon excitation is the sharp dip in the reflection curve around $\theta_{int} = \theta_{plasmon} = 43.9061$. The corresponding incident angle would be $\alpha = 26.5924^\circ$. Where as the theoretical angle of plasmon would be 43.0127° . Errors in the results can will be discussed later.

1.3.3 SPR (Method-B)

Figure 1.6 presents the results obtained with Method-B. Super continuum laser was used and the reflected beam was detected in spectrometer at the incident angle ($\alpha = 26.5924^\circ$) as it was plasmon angle, calculated in above section.

Now taking one step further and measuring the shift of dip as the angle of incidence

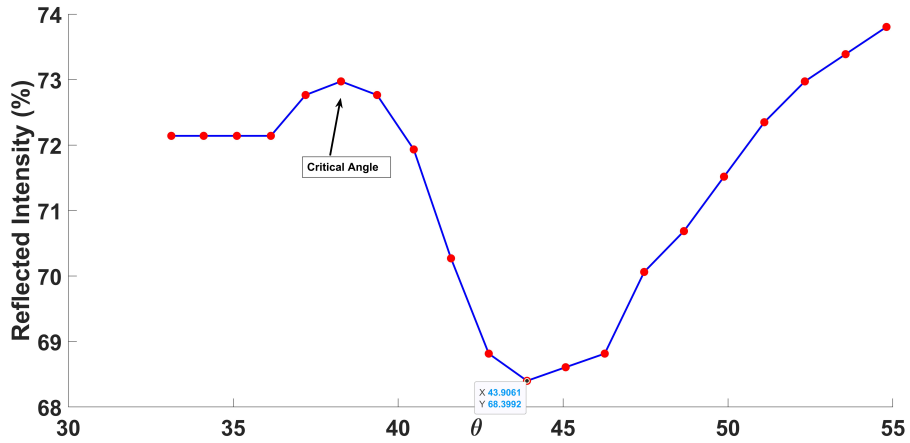


FIGURE 1.5: Surface plasmon extinction curve for a gold/air interface measured at a wavelength of 633nm. The graph shows the reflected intensity plotted versus θ_{int} as obtained with relation 1.6

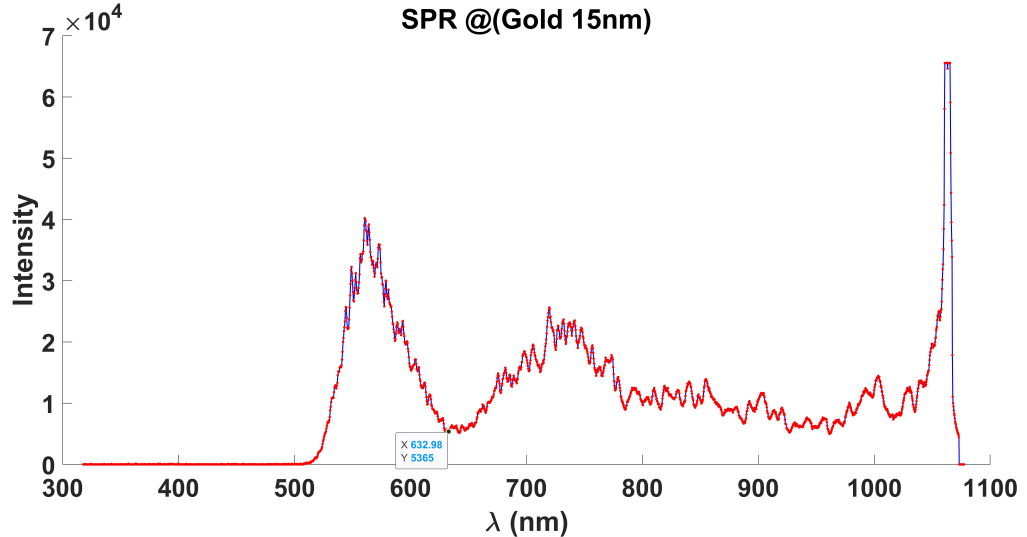


FIGURE 1.6: Surface plasmon extinction curve. The graph shows the reflected intensity plotted versus λ at the incident angle ($\alpha = 26.5924^\circ$)

changes. From equation 1.6 it is clear that for the change in the angle L.H.S. something in the R.H.S. has to compensate, that something is $\epsilon_1(\omega)$. That will change the refractive index of metal and a different wavelength will be absorbed. Figure 1.7 shows the absorption of different wavelengths. Based on the absorption we have plotted the incident angle(α) vs wavelength(nm)(Figure 1.8) for both theoretical prediction and experimental observation.

As the incident angle will change to compensate the effect $\epsilon_1(\omega)$ will change according to equation 1.1. This implies the absorption of different wavelength(Data from ref.[2] used for the refractive index of gold at different wavelength). In Figure 1.7 red colour curve shows the spectrum at $\alpha = 60^\circ$, blue colour shows the spectrum at $\alpha = 58^\circ$ and absorption of 566.96nm wavelength, green colour shows the spectrum at $\alpha = 56^\circ$ and

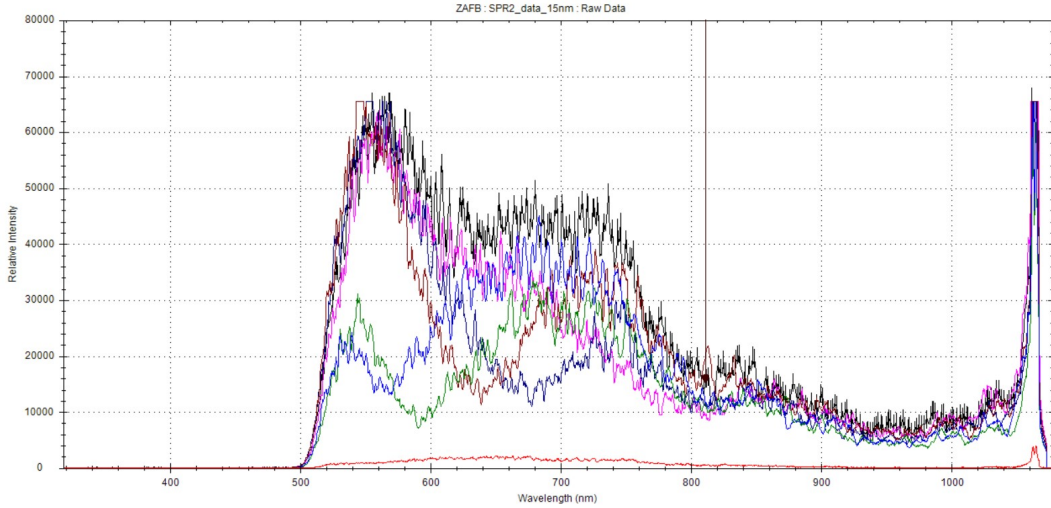


FIGURE 1.7: Surface plasmon extinction curve. The graph shows the reflected intensity plotted versus λ at the different incident angle

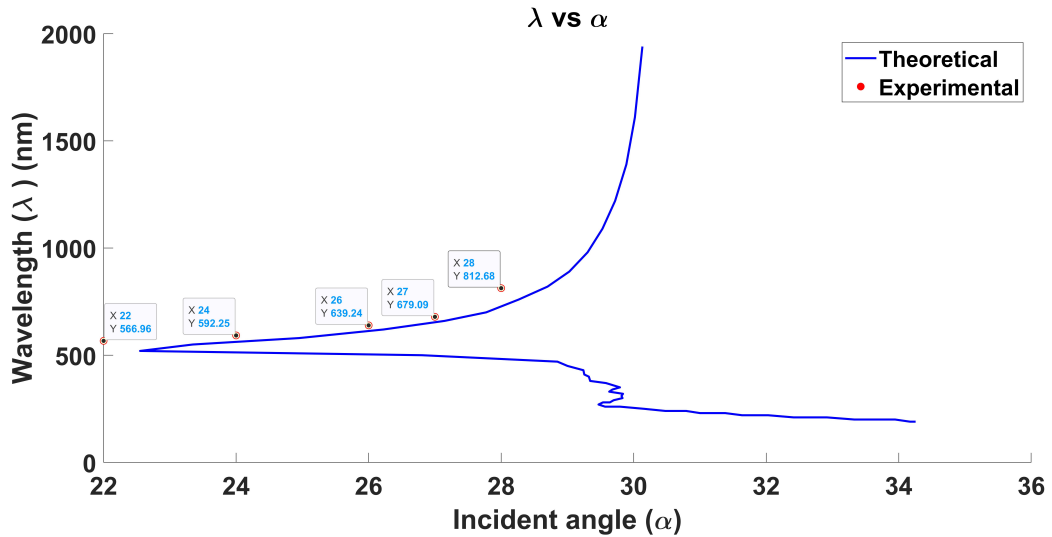


FIGURE 1.8: λ vs the incident angle (α). Blue line shows the theoretical plot(ref.[2]) where as red data points shows the experimental results.

absorption of 592.25nm wavelength, dark red colour shows the spectrum at $\alpha = 54^\circ$ and absorption of 639.24nm wavelength, dark blue colour shows the spectrum at $\alpha = 53^\circ$ and absorption of 679.09nm wavelength, magenta colour shows the spectrum at $\alpha = 52^\circ$ and absorption of 812.68nm wavelength, and black colour shows the spectrum at $\alpha = 50^\circ$.

1.3.4 Sources of Error

- Non Homogeneous distribution of gold film thickness.
- Rough and scratch surface of gold film.
- Untrained handling of gold film.
- Mismatch between refractive index of prism and glycerin.

- Moisture and dust accumulation on the gold-air interface.

1.4 Conclusion

We described a series of experiments designed to provide insights into the fundamental properties of surface plasmon resonance in this report. An important part of the experiment involves the excitation of the plasmon resonance by using a He–Ne laser in the Kretschmann configuration, with the gold active film embedded in a prism of glass. An accurate measurement of the plasmon extinction angle is performed and the measurement is compared to the theoretical prediction. Further verification of momentum conversation form equation 1.6 is illustrate in Figure 1.8.

Good amount of time was spent into to find out the difficulties in observing the SPR and to reach at the conclusion that one of the given gold film was damaged or not smooth enough to excite the SP wave. Gold-water interface SP excitation was also attempted but resulted in unsuccessful as the gold film got damaged during the process of setting up the experiment.

As the wavelength shifts from red to blue, the coupling between gold's surface plasmon wave and the interband transitions results in damping of the resonance. A good illustration of the electromagnetic principles at work in SPR can be obtained by using this setup, which is easy to adjust and handle.

Chapter 2

Tamm Plasmon

2.1 Theory

The symmetry between the periodic potential in Condensed Matter Physics and its optical analogue in terms of alternate layers of different refractive indices can be exploited to develop a theoretical framework in which computational modelling and subsequent experimentation can be done. For this purpose, DBR is used as the Photonic Crystal.

2.1.1 Optical Tamm states (OTSSs)

To begin with, Tamm states are electronic surface energies that are predicted to be localized on crystal surfaces. Optical Tamm states (OTSSs) are surface modes that are generated by perturbing properly periodic optical impedance at the surface of PhC. Opposing surface plasmon modes that are confined along an interface between a dielectric and a conductor, OTSSs have a smaller wave vector (parallels to the interface) than

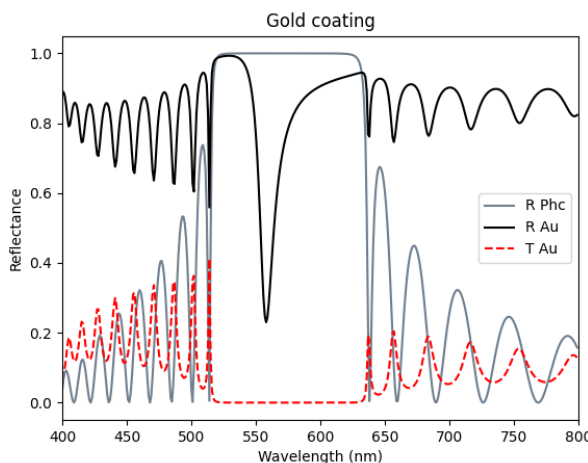


FIGURE 2.1: imulated spectrum of metal coating on PhC formfigure.... configuration. Reflection (Black curve), transmission (Red curve) and PhC reflection (Grey curve) curves

light waves in a vacuum. It enables a direct optical excitation of such modes for both transverse magnetic (TM) and transverse electric (TE) incident polarisation.

Studying the reflectivity and transmittivity spectra, Tamm states in a metal-PhC can be identified. In the spectra given in Figure 2.1, the grey plot is that of reflectivity when no metal coating is there. The reflectivity (shown in black color) increases as expected when metal is coated, but at 560nm , in the photonic band gap, dip in reflectivity is observed. At this wavelength the transmittivity(in red colour) is almost vanishing. This allows us to infer that particular state has a localized field distribution inside the metal-PhC system. Thus the state at 560nm is identified as a Tamm state. Field intensity distribution at this wavelength is localized at the interface of then metal and PhC.

2.2 Experimental Setup

Experimental setup is described in the Figure 2.2.

2.2.1 Apparatus

- White light source
- Polarised beam splitter
- Collimating convex lens
- Aperture
- DBR and gold coated DBR
- Rotating stage
- Optical fiber cables
- Spectrometer

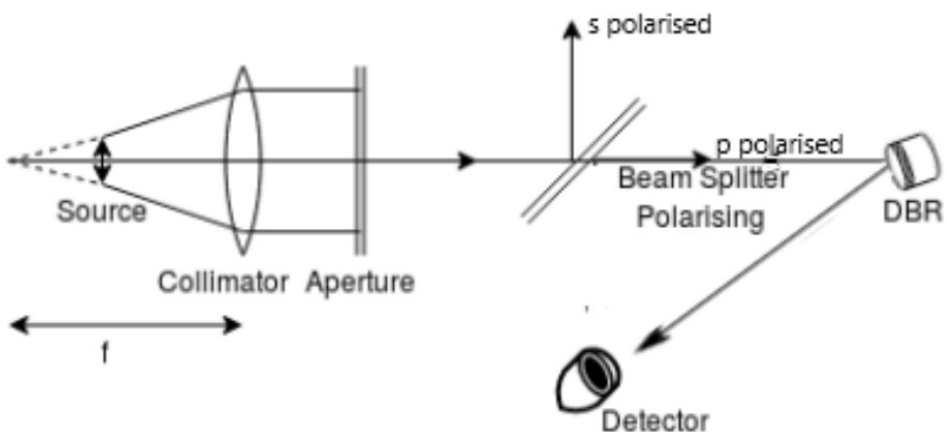


FIGURE 2.2: Experimental setup for the observation of Tamm states

There is NO point source of white light; it consists of diverging beams instead. A parallel light beam is formed by collimating a convex lens whose focal length is at a distance from the focal length of a virtual point source to get a homogeneous intensity by opening an aperture. Now, this light is passed through a Polarising beam splitter, which splits the original beam into two beams, polarised s and polarized p. This light is then passed through the DBR, which is then positioned in the path of either polarized light. Following that, the reflected light from the DBR is made to fall on the detector, where it travels through the optical cable to the spectrometer that is connected to the laptop, and a plot in BWSpec software is obtained.

2.3 Results and Discussion

2.3.1 Tamm plasmon for p-polarised light

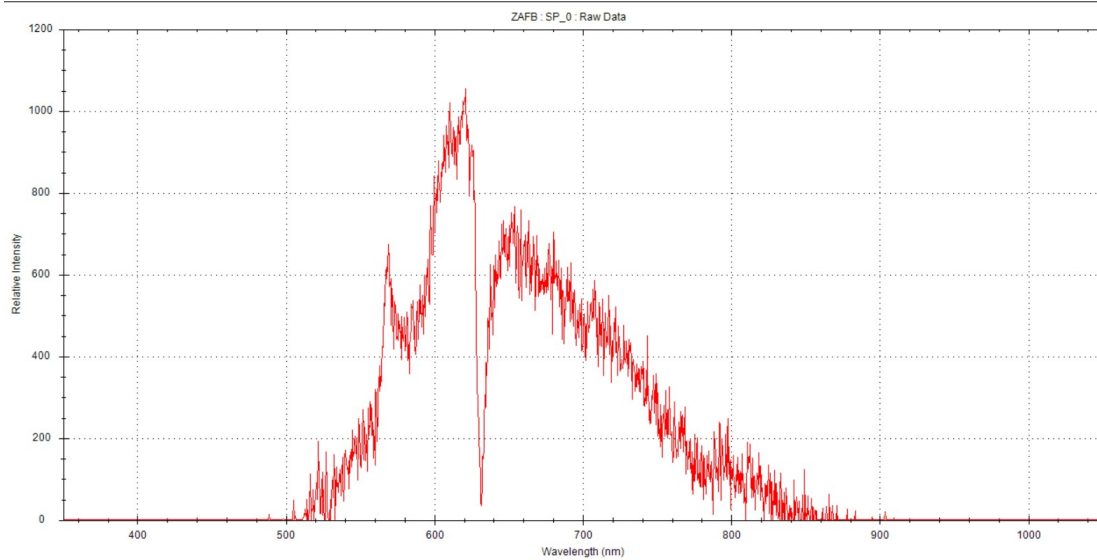
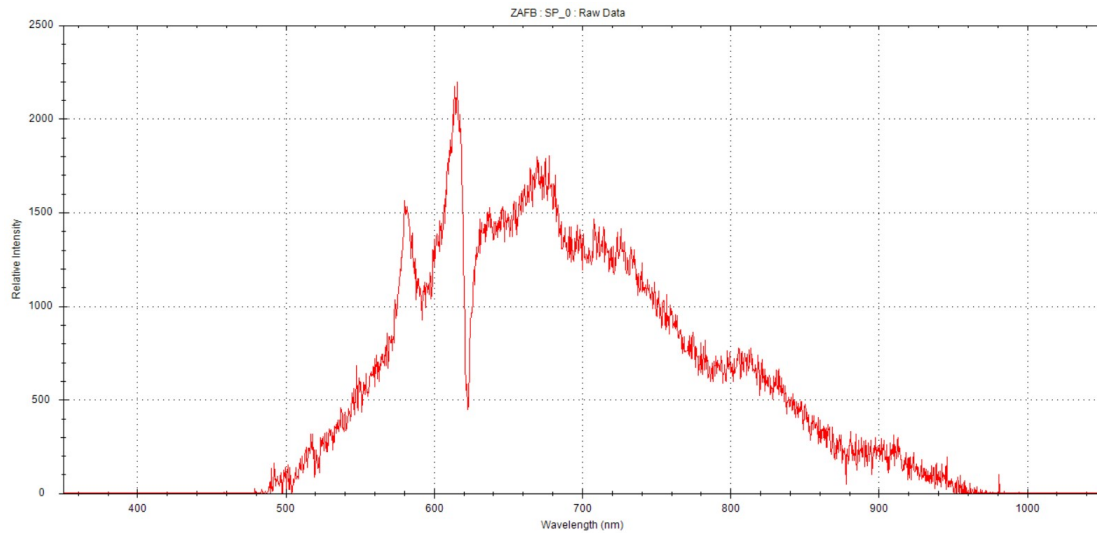
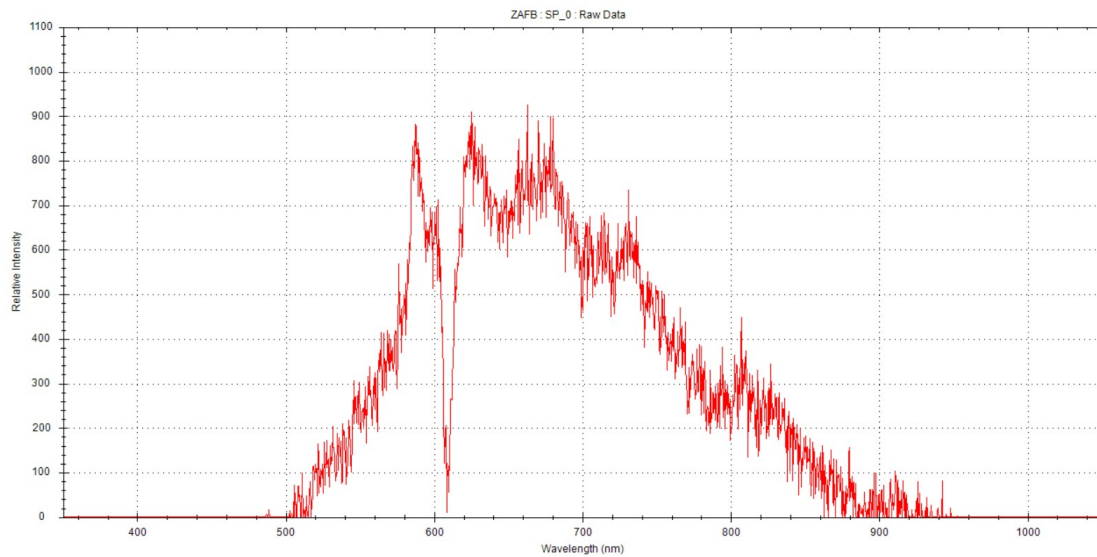
the metal-coated DBR (30 nm Au) is placed on a rotating base and the Polarising Beam splitter is used. The transmitted light from the Beam-splitter is p-polarised while the reflected light is s-polarised. Thus the spectrometer and the DBR are placed in path of p-polarised light. Results are appended form Figure [2.3 to 2.7](#)

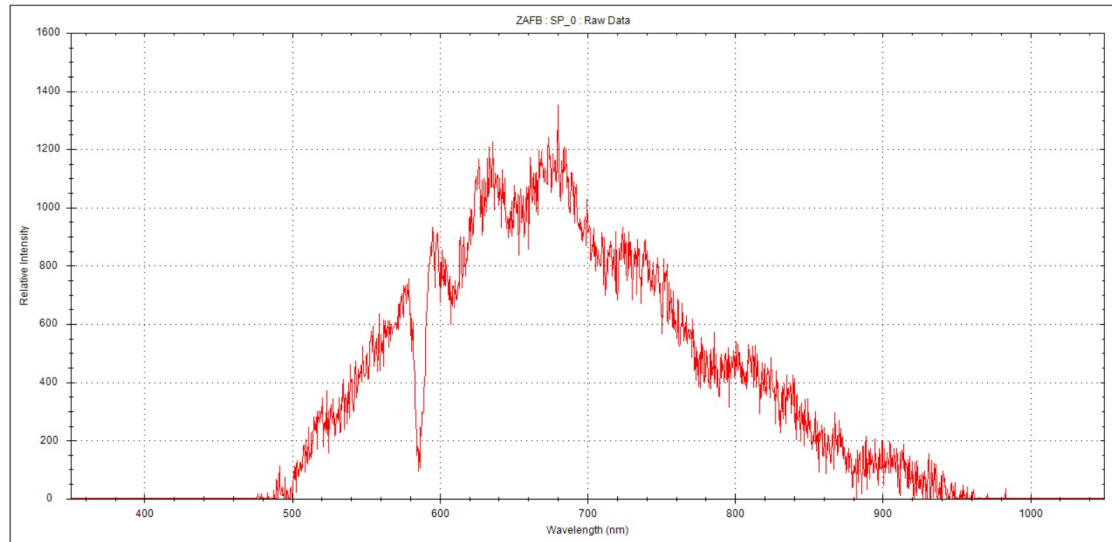
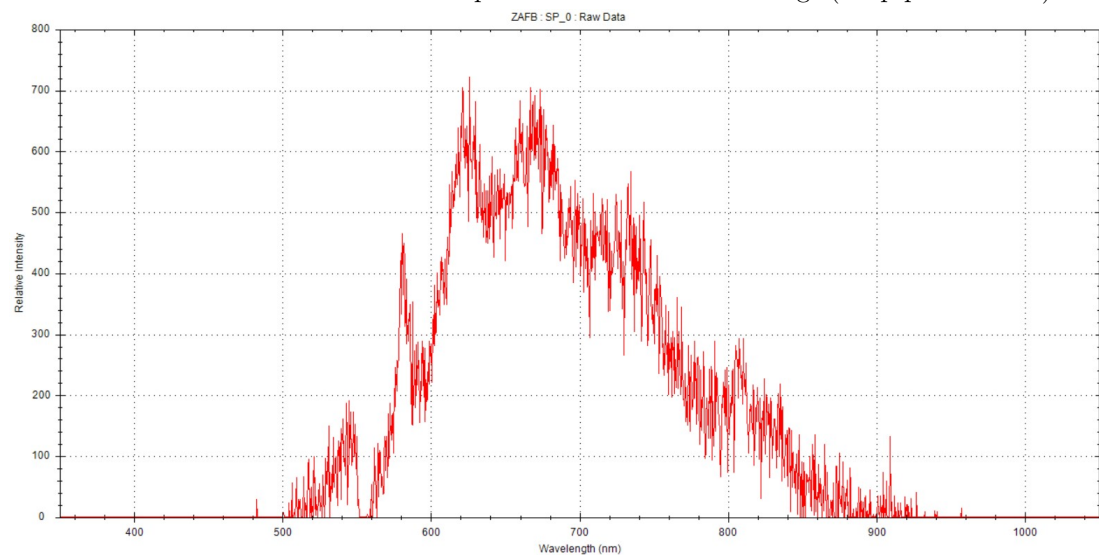
2.3.2 Tamm plasmon for s-polarised light

the metal-coated DBR (30 nm Au) is placed on a rotating base and the Polarising Beam splitter is used. The transmitted light from the Beam-splitter is p-polarised while the reflected light is s-polarised. Thus the spectrometer and the DBR are placed in path of s-polarised light. Results are appended form Figure [2.8-2.11](#).

2.4 Conclusion

We describe a series of experiments designed to provide insights into the fundamental properties of Tamm plasmon in this report. We have simulated the DBR spectra, bandgap, and its variation with the angle of incidence. Stepping ahead, metal coated DBR was also simulated and results are presented in the pre-mid semester report. Here we observed the Tamm states via setting up the experiment. Tamm plasmon is different from SPR in a way that it can be observed for both s and p-polarised light where as SPR is only observed for p-polarisation. Hence the intensity for the spectrum of wavelength is observed for increasing angle. The simulated results matched with the one experimentally. Both by simulation and experimentation we conclude that the Tamm resonance wavelength decreases with increase in the angle of incidence. This experiment was quite easy to perform as the setup and its procedure is already established. These measurements were taken when water-gold interface experiment setup was pending in the workshop, as a smart utilization of provided time.

FIGURE 2.3: Metal coated DBR spectrum for 10° incident angle(for p-polarization)FIGURE 2.4: Metal coated DBR spectrum for 20° incident angle(for p-polarization)FIGURE 2.5: Metal coated DBR spectrum for 30° incident angle(for p-polarization)

FIGURE 2.6: Metal coated DBR spectrum for 40° incident angle(for p-polarization)FIGURE 2.7: Metal coated DBR spectrum for 50° incident angle(for p-polarization)

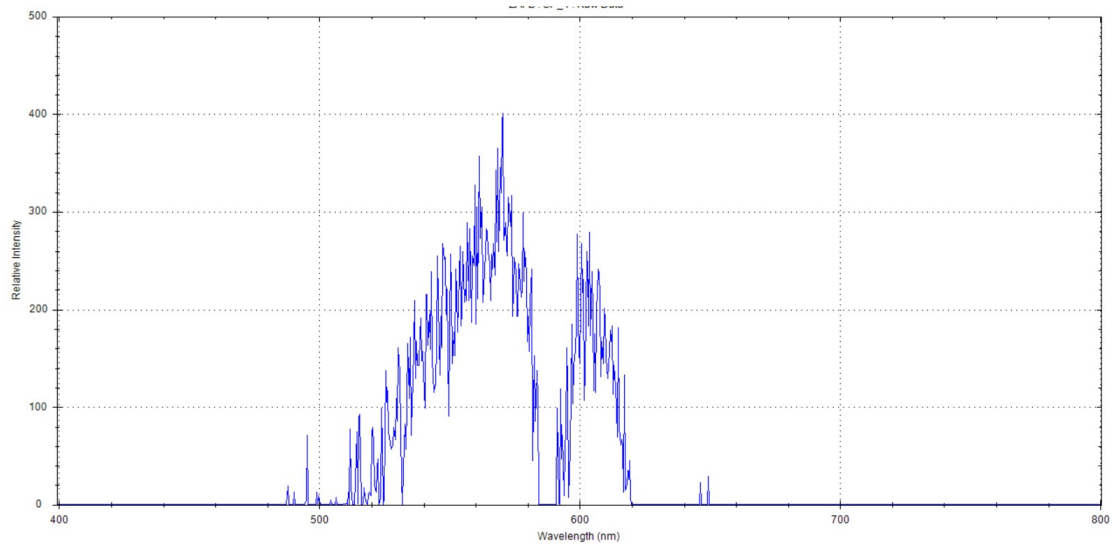


FIGURE 2.8: Metal coated DBR spectrum for 20° incident angle(for s-polarization)

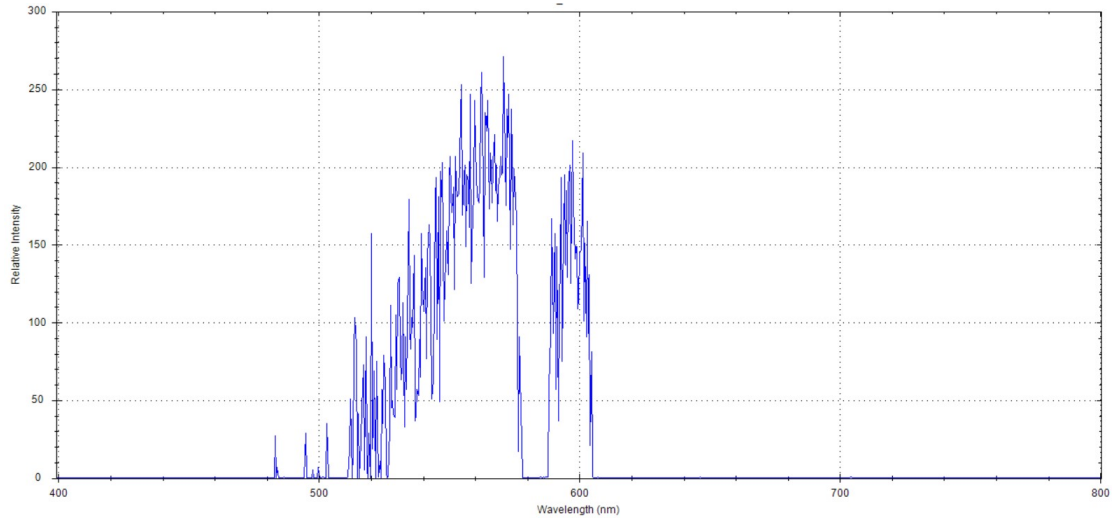


FIGURE 2.9: Metal coated DBR spectrum for 30° incident angle(for s-polarization)

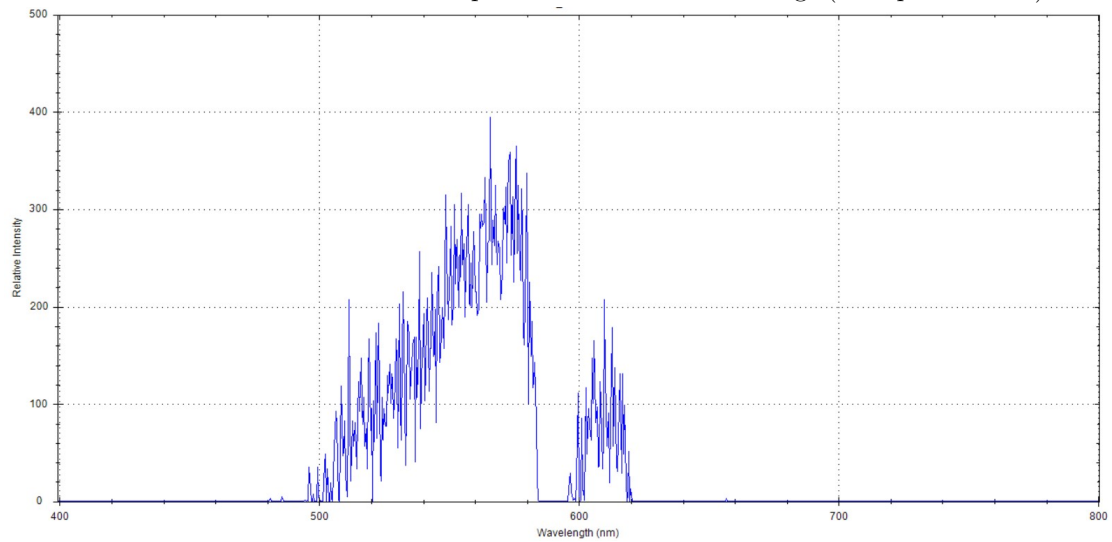


FIGURE 2.10: Metal coated DBR spectrum for 40° incident angle(for s-polarization)

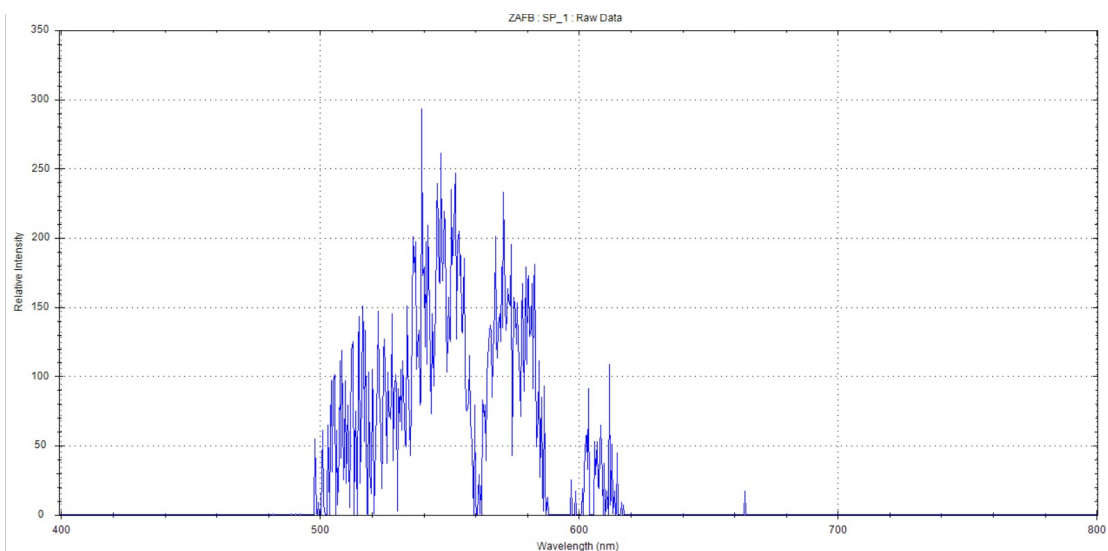


FIGURE 2.11: Metal coated DBR spectrum for 50° incident angle(for s-polarization)

References

- [1] Danni Hao. Hybridisation of plasmonic and acoustic biosensing devices. (1), 2017. URL <http://theses.gla.ac.uk/8992/>.
- [2] P. B. Johnson and R. W. Christy. Optical constants of the noble metals. *Physical review B*, (1), 1972. URL <https://journals.aps.org/prb/abstract/10.1103/PhysRevB.6.4370>.
- [3] J.C.B Longen. Interaction of lasers with plasmon resonance (lspr) coatings manipulation of au nanoparticles. *Eindhoven University of Technology*, (1), 2011. URL <https://research.tue.nl/en/studentTheses/interaction-of-lasers-with-plasmon-resonance-lspr-coatings>.
- [4] Romain Vayron Olivier Pluchery and Kha-Man Van. Laboratory experiments for exploring the surface plasmon resonance. *IOP Science*, (1), 2011. URL <https://iopscience.iop.org/article/10.1088/0143-0807/32/2/028>.
- [5] Katherine A. Willets and Richard P. Van Duyne. Localized surface plasmon resonance spectroscopy and sensing. *Rev. Phys. Chem.*, (1), 2007. doi: 10.1146/annurev.physchem.58.032806.104607.